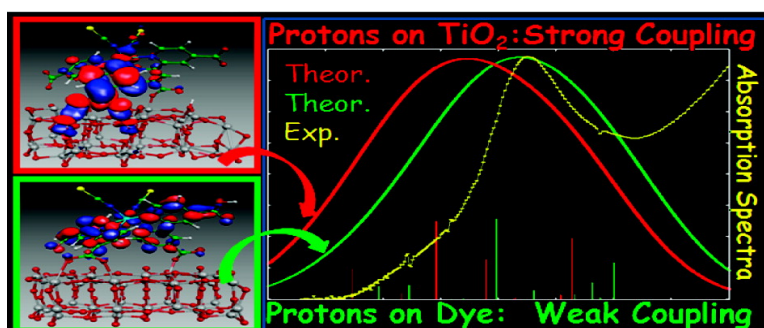


Time-Dependent Density Functional Theory Investigations on the Excited States of Ru(II)-Dye-Sensitized TiO Nanoparticles: The Role of Sensitizer Protonation

Filippo De Angelis, Simona Fantacci, Annabella Selloni, Mohammad K. Nazeeruddin, and Michael Grtzel

J. Am. Chem. Soc., **2007**, 129 (46), 14156-14157 • DOI: 10.1021/ja076293e • Publication Date (Web): 26 October 2007

Downloaded from <http://pubs.acs.org> on February 13, 2009



More About This Article

Additional resources and features associated with this article are available within the HTML version:

- Supporting Information
- Links to the 6 articles that cite this article, as of the time of this article download
- Access to high resolution figures
- Links to articles and content related to this article
- Copyright permission to reproduce figures and/or text from this article

[View the Full Text HTML](#)

Time-Dependent Density Functional Theory Investigations on the Excited States of Ru(II)-Dye-Sensitized TiO₂ Nanoparticles: The Role of Sensitizer Protonation

Filippo De Angelis,^{*,†} Simona Fantacci,[†] Annabella Selloni,[‡] Mohammad K. Nazeeruddin,[§] and Michael Grätzel[§]

Istituto CNR di Scienze e Tecnologie Molecolari (ISTM), c/o Dipartimento di Chimica, Università di Perugia, via Elce di Sotto 8, I-06123, Perugia, Italy, Department of Chemistry, Princeton University, Princeton, New Jersey 08544, and Laboratory for Photonics and Interfaces, Institute of Chemical Sciences and Engineering, School of basic Sciences, Swiss Federal Institute of Technology, CH-1015 Lausanne, Switzerland

Received August 21, 2007; E-mail: filippo@thch.unipg.it

Recently, much attention has been focused on dye-sensitized solar cells (DSSCs) as possible low-cost alternatives to conventional solid-state photovoltaic devices.¹ The most successfully employed charge-transfer sensitizers in DSSCs are Ru(II)-polypyridyl dyes,² which, adsorbed on nanostructured TiO₂ surfaces, yield solar-to-electric power conversion efficiencies of about 9–11% under AM 1.5 conditions.³ For Ru(II) dyes, the proposed DSSC mechanism involves photoexcitation to a dye excited state, from which an electron is transferred to the TiO₂ conduction band (*c.b.*).¹ This indirect injection mechanism is inferred from the similarity of the free dye absorption spectrum and that of the DSSC device.¹ For [Fe(CN)₆]⁴⁻ on TiO₂, on the other hand, direct photoexcitation to TiO₂ *c.b.* was suggested by appearance of a low-energy absorption band.^{4,5} The difference between the free and adsorbed dye absorption spectrum is therefore usually considered as an indication of the electron injection mechanism in DSSCs.

The main factors determining the DSSC efficiency are the photocurrent density, i_{ph} , related to the rate of electron injection to the semiconductor *c.b.*, and the open circuit potential, V_{OC} , which is related to the energy difference between the semiconductor *c.b.* edge and the mediator redox potential.¹ In an effort to optimize the overall device conversion efficiency,^{3,6} it was found that i_{ph} (V_{OC}) significantly increases (decreases), by increasing the number of protons carried by the sensitizer's carboxylic groups, which are used to anchor the dye onto the TiO₂ surface. Optimal performances were obtained for dyes carrying 0.5–2 protons over a possible range of 0–4.^{3,6} Since some of the sensitizer's protons can be transferred to the TiO₂ surface,⁶ these findings suggest that protonation of the sensitizer and/or of the surface can have an important influence on the electronic dye/semiconductor coupling (i_{ph}) and on the position of the TiO₂ *c.b.* (V_{OC}) in DSSCs.

A detailed understanding of the factors influencing i_{ph} and V_{OC} is essential to improve the performance of DSSC devices. To obtain such an understanding for the role of dye protonation, we have carried out fully first principles quantum mechanical calculations on the ground and excited states of the [*cis*-(NCS)₂-Ru(II)-bis(2,2'-bipyridine-4,4'-dicarboxylate)] dye, N719, adsorbed onto a model TiO₂ nanoparticle. In contrast to the extensive experimental work on DSSCs^{1–4,6} and numerous computational studies of Ru(II) sensitizers,⁷ so far only a few theoretical investigations of transition metal dyes on TiO₂ have been reported.^{5,8} Our nanoparticle model is represented by a stoichiometric anatase Ti₃₈O₇₆ cluster of nanometric dimensions exposing the majority (101) surface.⁹ Previous calculations by our group based on time-dependent density functional theory (TDDFT) have shown that the band gap of such a cluster in aqueous solution is ~3.2 eV,⁵ in excellent agreement with typical experimental values (3.2–3.3 eV).^{4,10} We optimized

the structure of N719 adsorbed onto TiO₂ by the Car–Parrinello (CP) method,¹¹ using the PBE functional.¹² To investigate the dye protonation effects, we considered the extreme cases in which the two protons initially carried by the dye are retained on the dye (A) or are both transferred to the TiO₂ nanoparticle (B); see Figure 1. This allows us to directly compare systems with the same charge and number of atoms, so that the effects of the TiO₂ cluster size and surface hydration (not explicitly included in our calculations) should be relatively unimportant. The same model has been recently used by us to investigate the effects of the sensitizer's adsorption mode on the DSSC V_{OC} .¹³ The semi-local PBE functional is known to underestimate the TiO₂ band gap,¹⁴ so for TDDFT excited state calculations, we used the hybrid B3LYP functional.¹⁵ In this case, 3-21G* and DVZP basis sets were used [see Supporting Information (SI)], adding solvation effects by C-PCM,¹⁶ as implemented in Gaussian03.¹⁷ Solvation effects are essential for describing the dye excited states;^{3,7d} we found only minor differences by including explicit water molecules solvating the dye in conjunction with C-PCM.³ We calculated the lowest 10 singlet excitations, thus simulating a large portion of the absorption spectrum and gaining insight into the dye/TiO₂ coupling.

The optimized geometries of the A and B configurations are reported in Figure 1. We find adsorption to take place via two carboxylic groups residing on different bipyridines, whereas an adsorption configuration via a single bipyridine was considered for the tetraprotonated dye.^{8a} Configuration B is 36.7 kcal/mol more stable than A; although probably overestimated, this value suggests that protons can be effectively transferred from the dye to the surface. For both A and B, the computed electronic structure shows that the N719 HOMOs, of mixed Ru–NCS character,^{3,7} fall within the TiO₂ band gap; the HOMO/HOMO-6 correspond to those of the isolated sensitizer, with the top of the TiO₂ valence band lying at lower energy (see SI). By contrast, significant differences between the A and B configurations are found in the energy and character of the LUMOs. In particular, adsorption of the two protons onto the TiO₂ surface in B leads to a LUMO downshift by about 0.15 eV compared to A, consistent with the experimentally found 270 mV V_{OC} reduction measured for DSSCs employing dyes containing 0–2 protons.^{3,6} In addition, despite being slightly sensitive to the basis set quality (see SI), our results unambiguously show that, associated to this energy downshift, there is a considerable mixing of the sensitizer π^* orbitals, delocalized across the carboxylic-substituted bipyridine ligands,^{3,7} with *c.b.* states of the TiO₂ nanoparticle (see Figure 2). While in A the LUMO/LUMO+1 are pure N719 π^* orbitals followed at higher energy by pure TiO₂ *c.b.* states (Figure 2), in B the LUMO/LUMO+3 are mixed N719/TiO₂ states.¹³

A comparison between the calculated absorption spectra for A and B and experiment³ for N719-sensitized DSSCs is reported in

[†] ISTM-CNR Perugia.

[‡] Princeton University.

[§] Swiss Federal Institute of Technology.

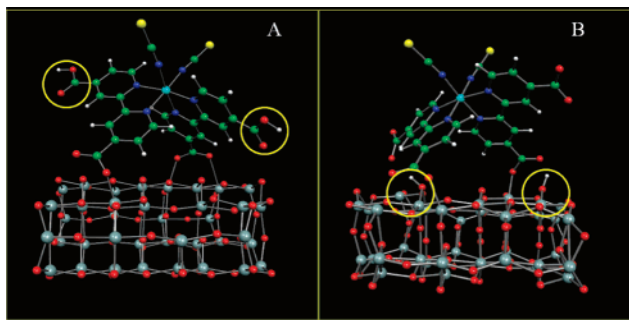


Figure 1. Optimized A and B structures of the N719 dye on the $(\text{TiO}_2)_{38}$ cluster. The yellow circles indicate the position of the two protons.

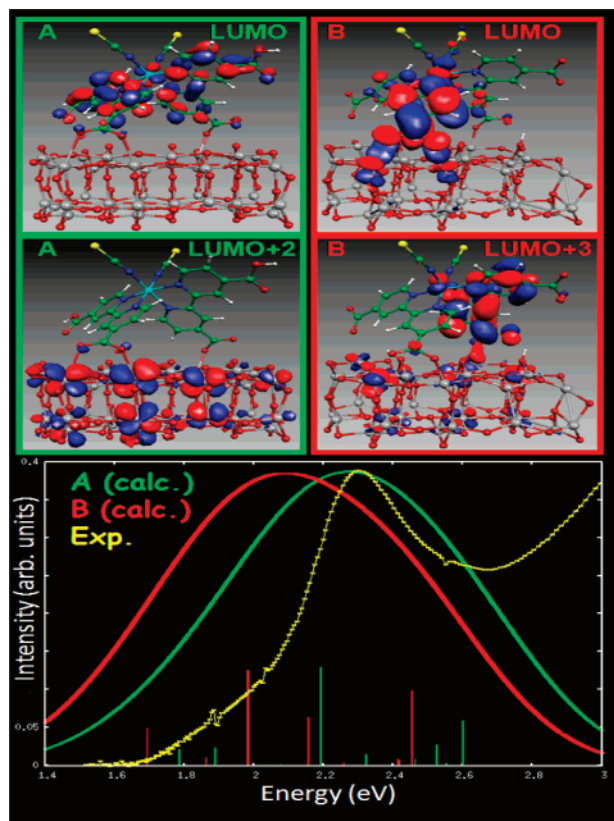


Figure 2. Top: plots of relevant LUMOs for A (left) and B (right). Bottom: comparison between computed absorption spectra for A (green) and B (red) and experiment for N719-sensitized DSSCs (yellow). Vertical lines indicate the calculated excitation energies and oscillator strengths. A Gaussian broadening with $\sigma = 0.25$ eV was used to simulate the theoretical spectra. The spectra have been rescaled to show the same peak intensity.

Figure 2. The spectral shapes calculated for A and B do not show significant differences and, although slightly red-shifted and broader, are both in good agreement with the experiment. For A, the lowest singlet transition is of HOMO–LUMO character, calculated at 1.78 eV; the absorption spectrum is dominated by an intense transition at 2.19 eV involving excitation from the HOMO-2/HOMO-1 to the LUMO/LUMO+1 and essentially corresponding to the dominant MLCT transition of N719 in solution, found at 2.38 eV (see SI). The resulting excited state is only weakly energetically and spatially coupled to the TiO_2 *c.b.*, thus a reduced rate of electron injection from the dye to TiO_2 is to be expected.¹⁸ For B, the lowest singlet transition is found at 1.69 eV, again of HOMO–LUMO character; the absorption spectrum is characterized in this case by two main excitations at 1.98 and 2.45 eV, starting both from the dye HOMOs to the LUMO and LUMO+3, respectively. The latter are mixed-dye TiO_2 states, indicating that in B the dye excited states

are strongly coupled to the TiO_2 *c.b.*, giving rise to large rates of electron injection.

In conclusion, our study confirms an injection mechanism for Ru(II) dyes on TiO_2 mediated by the dye excited states and indicates a remarkable effect of dye protonation on the electronic properties of N719-sensitized TiO_2 nanoparticles. We find that two different electron injection mechanisms may be present in DSSCs employing dyes carrying a different number of protons: the strong coupling of the dye/ TiO_2 excited states computed upon TiO_2 protonation suggests that an adiabatic injection mechanism, in which the same electronic state changes its localization from the dye to the TiO_2 ,¹⁸ might be responsible of the high rates of electron injection observed experimentally for Ru–polypyridyl dyes on TiO_2 .^{1–3} For Ru dyes containing no protons, on the other hand, a nonadiabatic electron injection mechanism, in which the photoexcited electron tunnels from the dye to the TiO_2 *c.b.*, seems most likely, due to the lack of strong coupling between the dye/ TiO_2 . Despite such differences, the calculated absorption spectra corresponding to strongly and weakly coupled dye/ TiO_2 excited states are remarkably similar, so that a discrimination of the two electron injection regimes seems not to be feasible based on inspection of the absorption spectra.

Acknowledgment. F.D.A. and S.F. thank MIUR (FIRB 2003: Molecular compounds and hybrid nanostructured materials with resonant and non resonant optical properties for photonic devices) and CNR (PRIMO 2006) for financial support. Md. N. and M. G. thank the Swiss National Science Foundation and the Swiss Federal Office for Energy (OFEN) for financial support.

Supporting Information Available: Full reference 17, MO plots and energy diagrams, comparison between 3-21G*/DZVP results, N719 TDDFT results in solution, and excitation energies for A and B. This material is available free of charge via the Internet at <http://pubs.acs.org>.

References

- (1) (a) O'Regan, B.; Grätzel, M. *Nature* **1991**, *353*, 737. (b) Hagfeldt, A.; Grätzel, M. *Chem. Rev.* **1995**, *95*, 49. (c) Grätzel, M. *Nature* **2001**, *414*, 338.
- (2) Nazeeruddin, M. K.; Kay, A.; Rodicio, I.; Humphry-Baker, R.; Müller, E.; Liska, P.; Vlachopoulos, N.; Grätzel, M. *J. Am. Chem. Soc.* **1993**, *115*, 6382.
- (3) Nazeeruddin, M. K.; De Angelis, F.; Fantacci, S.; Selloni, A.; Viscardi, G.; Liska, P.; Ito, S.; Takeru, B.; Grätzel, M. *J. Am. Chem. Soc.* **2005**, *127*, 16835.
- (4) Yang, M.; Thompson, D. W.; Meyer, G. J. *Inorg. Chem.* **2000**, *39*, 3738.
- (5) De Angelis, F.; Tilocca, A.; Selloni, A. *J. Am. Chem. Soc.* **2004**, *126*, 15024.
- (6) Nazeeruddin, M. K.; Humphry-Baker, R.; Liska, P.; Grätzel, M. *J. Phys. Chem. B* **2003**, *107*, 8981.
- (7) See for example: (a) Rensmo, H.; Södergren, S.; Patthey, L.; Westmark, K.; Vayssieres, L.; Khole, O.; Brühwiler, P. A.; Hagfeldt, A.; Sieghban, H. *Chem. Phys. Lett.* **1997**, *274*, 51. (b) Monat, J. E.; Rodriguez, J. H.; McCusker, J. K. *J. Phys. Chem. A* **2002**, *106*, 7399. (c) Guillemoles, J.-F.; Barone, V.; Joubert, L.; Adamo, C. *J. Phys. Chem. A* **2002**, *106*, 11354. (d) Fantacci, S.; De Angelis, F.; Selloni, A. *J. Am. Chem. Soc.* **2003**, *125*, 4381.
- (8) (a) Persson, P.; Lundqvist, M. J. *J. Phys. Chem. B* **2005**, *109*, 11918. (b) Lundqvist, M. J.; Nilsing, M.; Lunell, S.; Akemark, B.; Persson, P. *J. Phys. Chem. B* **2006**, *110*, 20513.
- (9) Vittadini, A.; Selloni, A.; Rotzinger, F. P.; Grätzel, M. *Phys. Rev. Lett.* **1998**, *81*, 2954.
- (10) Weng, Y. X.; Wang, Y. Q.; Asbury, J. B.; Ghosh, H. N.; Lian, T. *J. Phys. Chem. B* **2000**, *104*, 93.
- (11) (a) Car, R.; Parrinello, M. *Phys. Rev. Lett.* **1985**, *55*, 2471. (b) Pasquarello, A.; Laasonen, K.; Car, R.; Lee, C.; Vanderbilt, D. *Phys. Rev. Lett.* **1992**, *69*, 1982. (c) Giannozzi, P.; De Angelis, F.; Car, R. *J. Chem. Phys.* **2004**, *120*, 5903.
- (12) Perdew, J. P.; Burke, K.; Ernzerhof, M. *Phys. Rev. Lett.* **1996**, *77*, 3865.
- (13) De Angelis, F.; Fantacci, S.; Selloni, A.; Grätzel, M.; Nazeeruddin, M. K. *Nano Lett.* **2007**, *7*, 3189.
- (14) Di Valentin, C.; Pacchioni, G.; Selloni, A. *Phys. Rev. Lett.* **2006**, *97*, 166803.
- (15) Becke, A. D. *J. Chem. Phys.* **1993**, *98*, 5648.
- (16) Cossi, M.; Barone, V. *J. Chem. Phys.* **2001**, *115*, 4708.
- (17) Frisch, M. J.; et al. *Gaussian 03*; see SI for complete reference.
- (18) Duncan, W. R.; Craig, C. F.; Prezhdo, O. V. *J. Am. Chem. Soc.* **2007**, *129*, 8528.

JA076293E